IEICE TRANS. FUNDAMENTALS, VOL.E91–A, NO.4 APRIL 2008

PAPER Special Section on Selected Papers from the 20th Workshop on Circuits and Systems in Karuizawa

Color Demosaicing Using Asymmetric Directional Interpolation and Hue Vector Smoothing

Yoshihisa TAKAHASHI[†a)], ***Student Member***, **Kentaro HIRAKI**[††], ***Nonmember***, **Hisakazu KIKUCHI**[†], ***Fellow***, ***and*** **Shogo MURAMATSU**[†], ***Member***

SUMMARY This paper presents a color demosaicing method applied to the Bayer pattern color filter array (CFA). Reliable estimation of an edge direction, edge-directed asymmetric interpolation, and the use of color samples at immediate neighbors are considered as the key guidelines for smooth and sharp image restoration. Also, special interest is directed to local areas that are rich in high spatial frequency variations. For suppression of false colors likely to occur in those areas, a hue vector representation is introduced so that the spatial correlation between different color components may be exploited in consistent with the local constant-hue principle. Smoothing is repeated in the hue vector field a few times. Experimental results have shown preferable performances in terms of PSNR, CIELAB color difference, hue angle difference, CIE chromaticity and visual appearance, in particular resulting in less false colors.

key words: *image processing, color demosaicing, interpolation, CFA*

1. Introduction

A single-chip imager is one of the core components for most of digital cameras. A color filter array (CFA) is used to sample primary colors onto the Bayer pattern [1]. On such a Bayer pattern mosaic image, green samples are populated twice as many as red and blue samples, and two thirds of dense color values are missing. The task of color demosaicing is thus to restore these missing color values for producing a full resolution color picture which is unknown.

There are many problems to be solved in color demosaicing such as false color, zipper effect, blurring effect and others. While many sorts of demosaicing algorithms [2]–[8] are available at present, there is still a strong demand for sharp and visually-pleasing imaging. Among them, Cok's constant hue-based interpolation (CHBI) is one of the greatest contributions in this topic. The hue of the color on an object surface is maintained to avoid abrupt changes in CHBI. In particular, interpolation formulae are constructed so as to keep ratios of R to G and B to G constant. Adaptive color plane interpolation (ACPI) proposed by Hamilton and Adams is one of the well-performing demosaicing methods and has a simple algorithm. In ACPI, interpolation orientation is selected so that missing samples are interpolated along edges. Wu and Zhang introduced a soft decision framework that is known as an effective technique in decoding digital data in wireless communications. In their primary-consistent soft decision (PCSD) [8], two estimates are computed on the hypothesis of either of a horizontal or a vertical edge, before one of them is chosen depending on their likelihoods. It resulted in a significant reduction in false color and zipper effect, while the overall fidelity in terms of PSNR is gained a little. There is another approach to color demosaicing which is characterized by iteration. Kimmel's two-step superresolution algorithm [6] is one of the leading works along this direction and keeps its computational complexity at a reasonable level.

In this paper, a different approach is tried to solve the problem for improving sharpness and for reducing undesirable artifacts. Our objectives are higher fidelity in visual appearance, smaller restoration errors and suppression of excessive blur in demosaiced images [9]–[12]. We restrict ourselves to apply asymmetric directional interpolation in use of immediate neighboring color values for sharpness. A hue vector field is defined by the relative displacement of sparse primary colors against a dense primary color so that the hue vector variations may not affect the local assumption of constant hue [13]–[15]. The initial estimation by the directional interpolation is followed by an iterative smoothing to reduce undesirable artifacts, in particular, in the areas where high frequency variations are dominant and are likely to cause false colors.

The rest of the paper is organized as follows. Section 2 describes a set of direction indicators for detecting the edge orientation. Section 3 describes the asymmetric directional interpolation along the direction of the smallest indicator. The hue vector smoothing is presented in Sect. 4. Experimental results are presented in Sect. 5, and conclusions follow.

2. Estimation of the Edge Direction

Missing color values on the Bayer CFA shown in Fig. 1 have to be interpolated to restore an unknown original picture. Since an edge in an image is formed by two different types of areas across it, color values are different from each other between two areas separated by the edge. Smooth variations in color values are only possible along an edge. Hence an important guideline for a better interpolation is to make the interpolation along edges rather than across them.

In short, our interpolation guidelines are the following

Manuscript received June 26, 2007.
Manuscript revised October 6, 2007.

[†]The authors are with the Department of Electrical and Electronic Engineering, Niigata University, Niigata-shi, 950-2181 Japan.
[††]The author is with Oki Data Corporation, Takasaki-shi, 370-8585 Japan.
a) E-mail: yoshi-ta@telecom0.eng.niigata-u.ac.jp

DOI: 10.1093/ietfec/e91–a.4.978

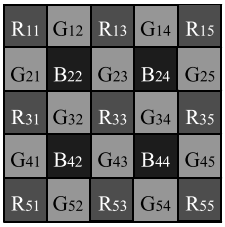

Fig. 1 Bayer CFA pattern.

four points.

- At first, edge directions are carefully detected around a local neighborhood.
- Secondly, the constant-hue property is assumed to be valid within individual local areas.
- Thirdly, the intensity variation along an edge can be asymmetric.
- Finally, immediate neighboring pixels are only used for interpolating missing color values in order to prevent from excessive blurring.

The direction of an edge at a particular pixel is estimated by investigating local gradients around the target pixel. Four color samples are available at the 4-connected neighboring pixels of a missing green value on the Bayer CFA shown in Fig. 1. In order to find the orientation of an edge, three direction indicators are formed by a collection of local gradients. If the missing green is located at the pixel (3, 3), the triple column direction indicator α is defined by

$$\alpha = \alpha_n + \alpha_c + \alpha_s \tag{1}$$

where

$$\alpha_n = |G_{12} - G_{32}| + |R_{13} - R_{33}| + |G_{14} - G_{34}|, \tag{2}$$
$$\alpha_c = |B_{22} - B_{42}| + |G_{23} - G_{43}| + |B_{24} - B_{44}|, \tag{3}$$
$$\alpha_s = |G_{32} - G_{52}| + |R_{33} - R_{53}| + |G_{34} - G_{54}|. \tag{4}$$

In the same way, the triple row direction indicator β is given by

$$\beta = \beta_w + \beta_c + \beta_e \tag{5}$$

where

$$\beta_w = |G_{21} - G_{23}| + |R_{31} - R_{33}| + |G_{41} - G_{43}|, \tag{6}$$
$$\beta_c = |B_{22} - B_{24}| + |G_{32} - G_{34}| + |B_{42} - B_{44}|, \tag{7}$$
$$\beta_e = |G_{23} - G_{25}| + |R_{33} - R_{35}| + |G_{43} - G_{45}|. \tag{8}$$

Although only column and row directions have been discussed in our previous research [9]–[12], we take diagonal directions into consideration in this paper[†]. The triple diagonal indicator is also defined over a 5 by 5 local area centered on the pixel of interest.

$$\gamma = \min(\gamma_{sw}, \gamma_{se}) \tag{9}$$

where

$$\begin{aligned}\gamma_{se} = {} & |G_{12} - G_{23}| + |G_{23} - G_{34}| + |G_{34} - G_{45}| \\ & + |R_{11} - R_{33}| + |B_{22} - B_{44}| + |R_{33} - R_{55}| \\ & + |G_{21} - G_{32}| + |G_{32} - G_{43}| + |G_{43} - G_{54}|, \end{aligned} \tag{10}$$
$$\begin{aligned}\gamma_{sw} = {} & |G_{14} - G_{23}| + |G_{23} - G_{32}| + |G_{32} - G_{41}| \\ & + |R_{15} - R_{33}| + |B_{24} - B_{42}| + |R_{33} - R_{51}| \\ & + |G_{25} - G_{34}| + |G_{34} - G_{43}| + |G_{43} - G_{52}|. \end{aligned} \tag{11}$$

If $\min(\alpha, \beta, \gamma) = \alpha$, it indicates that the vertical variation is smaller than the horizontal and diagonal variations, and thus a vertical edge is more probable to run across the location of interest.

3. Interpolation of Missing Color Values

It is a well-known fact that neighboring primary colors are closely correlated with each other. This generally observed knowledge on natural scene pictures was sophisticated into a constant-hue principle [2] over an object surface. Since green samples are populated twice as many as those of red and blue on the Bayer pattern, missing green values are at first interpolated, before missing red and blue values are interpolated with a help of dense green values.

On the other hand, the intensity variation along an edge is not always uniform along one direction and its opposite with respect to a target pixel to be interpolated. Directionally asymmetric interpolation along an edge is applied in this work, where less intensity variation is assumed to be of stronger significance in a sense of stable restoration for details. Choosing one of two opposite directions is of the strongest significance in such a sense. However it does not work well because of less information for balancing smoothness and sharpness in the interpolated images. Instead, directionally weighted interpolation is used for smooth interpolation and reference pixels are limited to immediate neighbors for the production of sharp images.

3.1 Interpolation of Missing Green Values

If $\min(\alpha, \beta, \gamma) = \alpha$, the missing value of g_{33} is interpolated along the vertical direction. According to the constant-hue principle, the hue variation is assumed to be small over neighboring pixels on an edge. If the hue variation is approximated by the difference between green and red, and if the unknown hue is interpolated by an average between the closest pair of hues along south to north, the following equation is obtained.

$$g_{33} - R_{33} = \frac{(G_{23} - r_{23}) + (G_{43} - r_{43})}{2} \tag{12}$$

where

[†]Note that the problem setting in this paper is completely different from that in Refs. [9], [10], [12]. Besides, several points have been improved; single Refs. [9], [10] to multiple Refs. [11], [12], where adaptive weighting has been introduced.

$$r_{23} = \frac{R_{13} + R_{33}}{2} \tag{13}$$

and

$$r_{43} = \frac{R_{33} + R_{53}}{2}. \tag{14}$$

In addition, we assume that less variation between a pair of opposite directions along an edge is significant so as to maintain continuous silhouette and stable sharpness around an edge. Hence we compute the asymmetric averaging as follows.

$$g_{33} = R_{33} + \frac{(1+\delta)(G_{23} - r_{23}) + (1-\delta)(G_{43} - r_{43})}{2} \tag{15}$$

where the adaptive weight is defined as

$$\delta = \frac{1}{2}\left(\frac{\alpha_s - \alpha_n}{\alpha_s + \alpha_n}\right) \tag{16}$$

which was constant in [9], [10].

If $\min(\alpha, \beta, \gamma) = \beta$, an edge is expected to run horizontally and the missing green value is interpolated as follows.

$$g_{33} = R_{33} + \frac{(1+\delta)(G_{32} - r_{32}) + (1-\delta)(G_{34} - r_{34})}{2} \tag{17}$$

where

$$r_{32} = \frac{R_{31} + R_{33}}{2}, \tag{18}$$

$$r_{34} = \frac{R_{33} + R_{35}}{2} \tag{19}$$

and

$$\delta = \frac{1}{2}\left(\frac{\beta_e - \beta_w}{\beta_e + \beta_w}\right). \tag{20}$$

If $\min(\alpha, \beta, \gamma) = \gamma$ including the case of $\alpha = \beta = \gamma$, Eqs. (15) and (17) are averaged for an estimate of the missing value.

3.2 Interpolation of Missing Red and Blue Values

Once all of missing green values have been interpolated, missing red and blue values are estimated with the help of dense green values. Since the missing color arrangements of red and blue are identical, it is enough to describe the interpolation for blue values. There are two different spatial arrangements for a missing blue value. In the first case, a missing blue value is sandwiched by a pair of blue samples along the vertical or horizontal orientation and the pair specifies the interpolation orientation. The interpolating formula for the sandwiched location along column or row is given by [10] as follows.

$$b_{23} = G_{23} + \frac{(B_{22} - g_{22}) + (B_{24} - g_{24})}{2} \tag{21}$$

$$b_{32} = G_{32} + \frac{(B_{22} - g_{22}) + (B_{42} - g_{42})}{2} \tag{22}$$

After these interpolations of the first case missing blue values have been completed, we compute the other missing blue values which are located at a face-centered position of four neighboring blue samples. The interpolating formula is of the form

$$b_{33} = g_{33} + \frac{(b_{32} - G_{32}) + (b_{34} - G_{34})}{2}. \tag{23}$$

4. Hue Vector Smoothing

False color and other visually-unpleasant artifacts can appear due to insufficient capability of the interpolation described in the previous section. On the other hand, the authors have observed that high frequency variations are strongly correlated among primary color values and it is invalid for low frequency variations [13], [14]. Based on this observation, it is a possible way to improve the restoration by exploiting the correlation among primary color values at particular areas where high frequency variations are dominant. In particular, we choose to modify hue values instead of color values so that the constant-hue principle may be kept well.

First of all, we define the hue vector H as follows.

$$H = \begin{pmatrix} h(1) \\ h(2) \end{pmatrix} = \begin{pmatrix} 1 & -1 & 0 \\ 0 & -1 & 1 \end{pmatrix} \begin{pmatrix} R \\ G \\ B \end{pmatrix} \tag{24}$$

The components of the vector are the primary color differences. They represent the relative displacements of a pair of primaries with respect to a reference primary of green, of which behavior is closest to the luma component in most cases. Also, the green samples are populated twice as many as the other primary color samples so that they are most reliable to convey fine spatial variations. The relative displacement allows us to maintain the local constant-hue principle, even if the hue vector may be varied in any ways and at any location.

The process of hue vector smoothing is initialized by defining an initial hue vector.

$$H^{(n)} = \begin{pmatrix} 1 & -1 & 0 \\ 0 & -1 & 1 \end{pmatrix} \begin{pmatrix} R \\ G \\ B \end{pmatrix} \tag{25}$$

where the iteration count n is set at zero.

Now a pixel location is tested if it belongs to high frequency variations. If the difference between the highest and lowest values of green samples within a local area exceeds a prescribed value, a high frequency variation is assumed to be dominant at that location. The local area is defined by a 3 by 3 square window centered on the target pixel in issue.

If a pixel of interest is present at such a location, a median hue vector is computed as follows.

$$H_m^{(n)} = \begin{pmatrix} h_m(1) \\ h_m(2) \end{pmatrix} \tag{26}$$

The median value components are computed within a 5 by

5 window centered on the target pixel. This is because median filtering offers effective lowpass filtering while keeping sharp transitions in spite of the presence of impulsive noises. It is followed by smoothing of the hue vector by the simplest linear interpolation.

$$H^{(n+1)} = \lambda H^{(n)} + (1-\lambda)H_m^{(n)} \tag{27}$$

The interpolation ratio is given by

$$\lambda = \frac{\omega_m}{\omega + \omega_m} \tag{28}$$

where ω is the minimum magnitude among four local gradients at the target pixel directed to its 4-connected neighbors on the present hue vector field. ω_m is the same but on the median-filtered hue vector field. For example, an explicit expression is given as follows, when location (2, 3) in Fig. 1 is of concern.

$$\omega = 1 + \min\Big(|h_{13}^{(n)}(1) - h_{23}^{(n)}(1)|, |h_{33}^{(n)}(1) - h_{23}^{(n)}(1)|, \\ |h_{22}^{(n)}(2) - h_{23}^{(n)}(2)|, |h_{24}^{(n)}(2) - h_{23}^{(n)}(2)|\Big), \tag{29}$$

where one is added just for avoiding zero-division.

The iteration count is incremented and the process is repeated a few times.

Once the iteration has been completed, we obtain a smoothed hue vector. It is equated to the hue vector representation of unknown primary color values.

$$\begin{pmatrix} r-g \\ b-g \end{pmatrix} = H^{(n+1)} \tag{30}$$

In order to reflect the modified hue vector onto three primary color values, we note that there exists a single known sample value among three values of r, g, and b. Hence any two missing primary color values, which are unknown, at a specific location are computed by solving the above linear equation system. For example, if a red sample is available at a location, missing green and blue values are found as follows.

$$\begin{aligned} g &= r - h^{(n+1)}(1) \\ b &= g + h^{(n+1)}(2) \end{aligned} \tag{31}$$

The resulting modification of primary color values is expectable to be consistent with the local constant-hue principle, as long as the local variations among primary colors are sufficiently correlated to each other.

5. Experimental Results

Experimental results are presented in two ways: visual inspection and objective evaluation. The number of iterations for hue vector smoothing has been set experimentally and three is large enough. The threshold value for detecting high frequency-dominant areas has been also set at seven through experiments.

5.1 Visual Inspection

Figure 2 shows a result of demosaicing of a geometric patterned image for visual inspection. Local fine views are displayed after magnification. Note that every step is equal to a pixel pitch. Most of false colors in Fig. 2 are yellow and cyan. False yellow means that color value interpolation is successful in red but fails in blue. The image restored by PCSD shows some undesirable artifacts at the crossing point at the center and at four corner edges. In contrast, the proposed method produces none of those artifacts, but ghost edges are weakly accompanied along diagonal edges.

Figures 3 and 4 are the results for natural scene pictures. Strong false colors are noticeable to the eye in ACPI-produced images. False colors are still observed in PCSD-produced images on casement windows, window glass corners and the water surface of the sea. In contrast, those artifacts are visually weak in the images restored by the proposed method.

Figure 5 is a visualization of Munsell hue difference measured on demosaiced images. The color space used for evaluation is Mathematical-Transform-to-Munsell color space [16] which is one of the most perceptually-uniform color spaces. The hue angle difference is displayed in $255 \times \sqrt{|\Delta H|/\pi}$ for a visualization purpose, where a large hue difference is displayed in bright grayscale. In the figure, part (c) shows a dark appearance that is an evidence of smaller hue difference between the original and a demosaiced image.

5.2 Objective Evaluation

Objective evaluations are developed with respect to Kodak 24 test image set shown in Fig. 6 that is the most widely used images in color demosaicing studies. PSNR is listed in Table 1 for a comparison among ACPI and PCSD, and the proposed method. As seen in the table, the proposed method

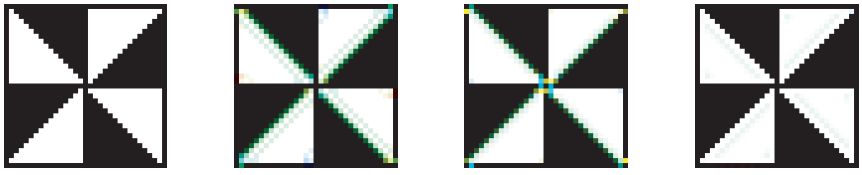

Fig. 2 Local fine views of interpolation. (a) Original. (b) ACPI. (c) PCSD. (d) Proposed.

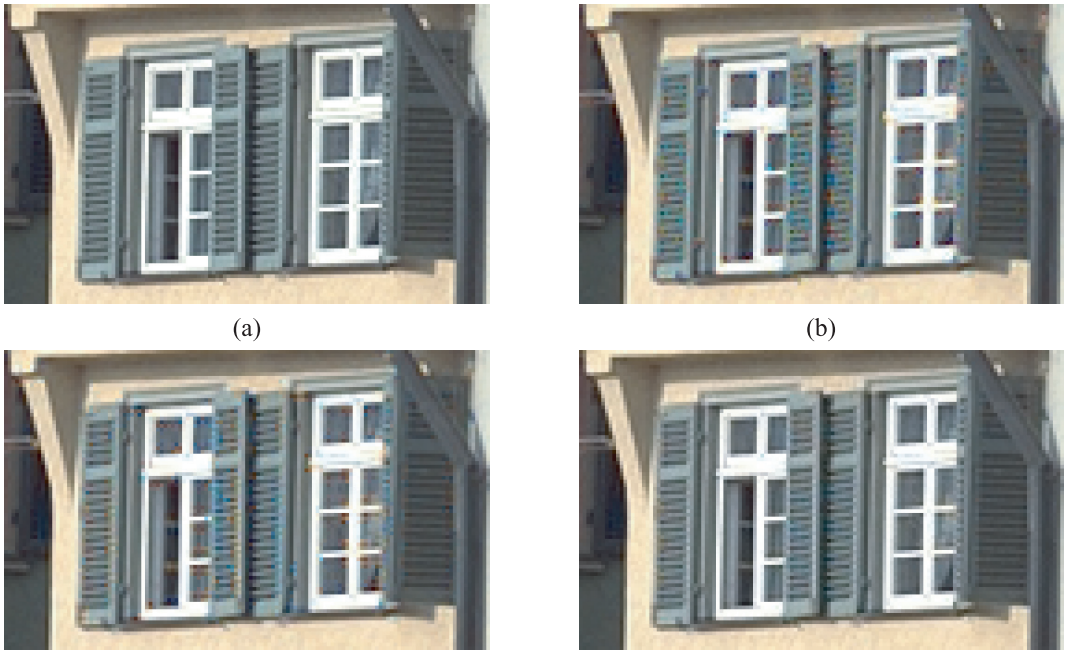

Fig. 3 Visual appearance of the color reproduction. A part of *town (Kodak set)*. (a) Original. (b) ACPI. (c) PCSD. (d) Proposed.

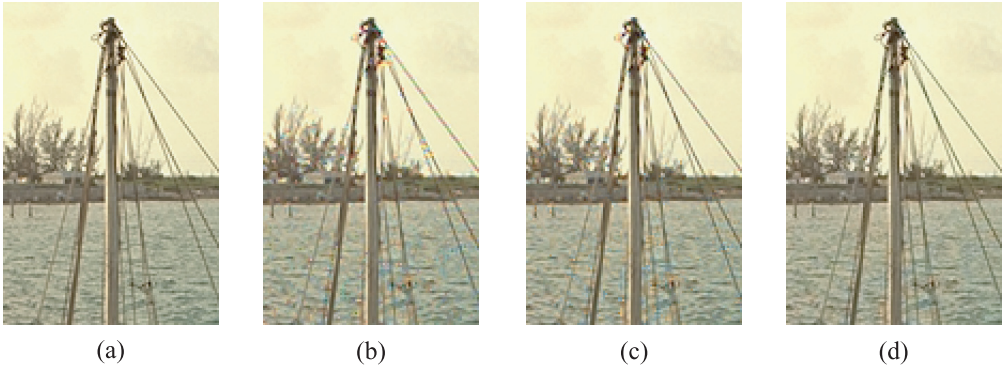

Fig. 4 Visual appearance of the color reproduction. A part of *zentime (Kodak set)*. (a) Original. (b) ACPI. (c) PCSD. (d) Proposed.

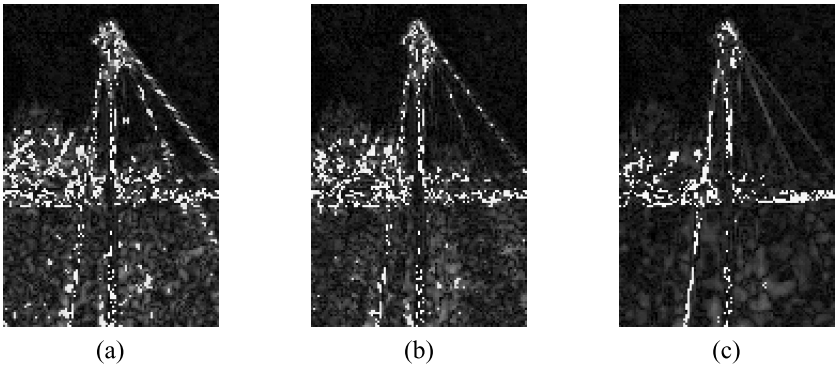

Fig. 5 Munsell hue difference. A part of *zentime (Kodak set)*. (a) ACPI. (b) PCSD. (c) Proposed.

Fig. 6 Kodak test image set.

Table 1 PSNR in dB on the Kodak set.

	Red			Green			Blue		
Image	ACPI	PCSD	Proposed	ACPI	PCSD	Proposed	ACPI	PCSD	Proposed
brick wall	33.26	33.41	38.72	34.83	35.66	42.52	33.35	33.52	39.27
knob on door	37.11	36.85	37.19	40.92	41.02	42.57	39.43	38.83	40.62
caps	40.28	40.85	41.56	42.29	43.52	44.10	39.86	40.05	40.81
red riding hood	37.67	37.55	37.44	40.75	41.05	41.90	39.63	39.64	41.22
motocross	34.83	35.25	37.17	36.03	37.16	40.16	34.44	34.69	36.37
zentime	34.90	36.61	40.00	36.21	38.53	43.04	34.36	35.73	38.38
window	40.67	40.21	41.01	42.26	42.33	43.49	39.92	39.32	39.61
town	31.77	32.09	35.81	33.58	34.70	39.91	31.76	32.13	36.26
sailboats	39.93	40.21	41.72	41.67	42.45	44.02	39.64	39.86	40.87
sailing	39.79	39.82	41.26	41.48	41.81	44.02	39.03	39.04	40.57
pier	35.72	36.09	38.70	37.31	38.46	42.69	36.11	36.61	40.04
beach	40.00	40.38	41.79	42.46	43.23	45.17	40.09	40.71	42.27
mountain stream	29.74	30.41	36.26	30.79	31.93	38.80	29.31	29.85	34.48
rafting	35.07	34.73	34.34	37.37	37.60	38.09	35.30	34.95	34.96
girl	35.86	35.96	36.23	39.50	40.25	41.52	37.46	38.03	39.55
sea	38.30	40.11	42.72	39.82	41.76	44.87	38.13	39.42	41.31
statue	38.82	38.59	41.13	39.56	39.93	43.15	37.91	37.60	39.68
lady	33.60	33.95	36.41	34.71	35.54	39.29	32.95	33.23	35.74
lighthouse	36.90	37.18	40.36	38.41	39.28	43.33	36.68	37.01	39.74
six-shooter	38.33	38.32	41.33	39.62	40.23	44.04	36.61	36.78	38.55
lighthouse view	35.10	35.34	39.86	36.40	37.32	42.82	34.61	34.76	38.28
rustic	36.01	35.68	36.92	37.98	38.21	39.77	35.82	35.56	36.85
parrots	41.18	41.14	41.10	43.54	44.14	44.60	41.74	41.84	41.91
red gable	32.35	32.99	34.15	33.45	34.76	37.40	30.55	31.10	32.84
Average	36.55	36.82	38.88	38.37	39.20	42.14	36.45	36.68	38.76

outperforms the others in every primary color reproduction.

In Table 2, CIELAB color difference, ΔE^*_{ab}, is shown in two statistical values of average and median. By literature [17]–[21] it is hard to perceive ΔE^*_{ab} smaller than 0.3, 0.6, 1.2, 2.3, 2.5 or 3.0. If it exceeds ten, the difference is too large for relative comparison to become insignificant [22] because of the definition of CIELAB color difference with respect to the purpose of differentiating Munsell color charts. The critical limit differs by literature, and of course depends on viewing conditions and the perceptual capability of individuals. Proposed method is found to produce quite small color difference.

Figure 7 shows an example of the hue difference histogram measured on the same image with Fig. 5 also in the MTM color space. Most of pixels have their hue difference from the original smaller than 30 degrees, which shows a clear contrast to the other methods of ACPI and PCSD.

Another aspect in color reproduction can be evaluated by comparing the color distribution in the CIE 1931 chromaticity diagram with ITU-R BT.709 primaries and white

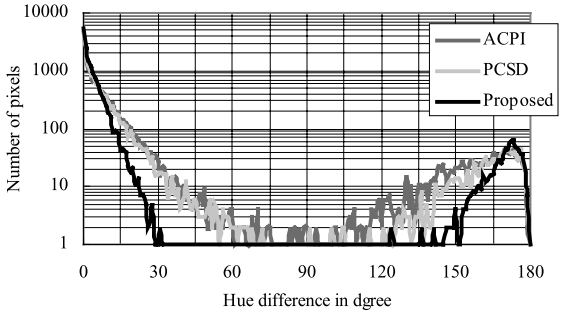

Fig. 7 Histogram of hue difference.

point. Figure 8 has been computed for image *mountain stream* and the triangle defines the ITU-R BT. 709 color gamut. It is observed that ACPI and PCSD make the color distributions spreaded in different colors that are not existent in the original image. In contrast, the color distribution reproduced by the proposed method is as compact as and closer to that of the original image. This is another evi-

Table 2 CIELAB color difference on the Kodak set.

	Average			Median		
Image	ACPI	PCSD	Proposed	ACPI	PCSD	Proposed
brick wall	3.16	2.89	1.73	2.36	2.12	1.40
knob on door	1.65	1.68	1.52	1.11	1.11	0.99
caps	1.21	1.12	1.00	0.78	0.77	0.73
red riding hood	1.67	1.64	1.49	1.20	1.18	1.06
motocross	2.72	2.47	2.01	1.79	1.66	1.40
zentime	2.32	1.91	1.49	1.45	1.28	1.14
window	1.32	1.32	1.27	0.84	0.84	0.82
town	3.34	3.10	2.20	2.16	2.04	1.64
sailboats	1.43	1.33	1.22	1.14	1.11	0.99
sailing	1.43	1.36	1.23	1.15	1.10	0.99
pier	2.06	1.85	1.44	1.29	1.19	1.10
beach	1.29	1.19	1.03	0.97	0.88	0.73
mountain stream	4.81	4.32	2.57	3.50	3.16	2.03
rafting	2.36	2.26	1.93	1.60	1.46	1.20
girl	1.79	1.72	1.52	1.11	1.09	0.97
sea	1.67	1.41	1.15	1.15	1.02	0.86
statue	1.59	1.53	1.25	1.16	1.13	0.94
lady	2.94	2.77	2.30	2.01	1.94	1.72
lighthouse	2.08	1.94	1.49	1.40	1.34	1.21
six-shooter	1.68	1.60	1.28	1.08	1.08	1.01
lighthouse view	2.42	2.23	1.60	1.44	1.39	1.23
rustic	2.25	2.20	1.99	1.53	1.50	1.42
parrots	1.17	1.15	1.11	0.89	0.89	0.83
red gable	2.73	2.52	2.09	1.36	1.31	1.18
Average	2.13	1.98	1.58	1.44	1.36	1.15

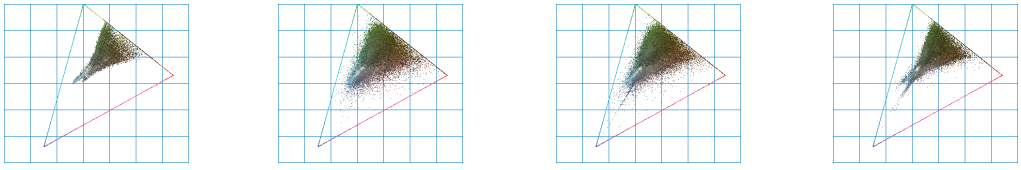

(a) (b) (c) (d)

Fig. 8 CIE 1931 chromaticity diagram of *mountain stream (Kodak set)*. (a) Original. (b) ACPI. (c) PCSD. (d) Proposed.

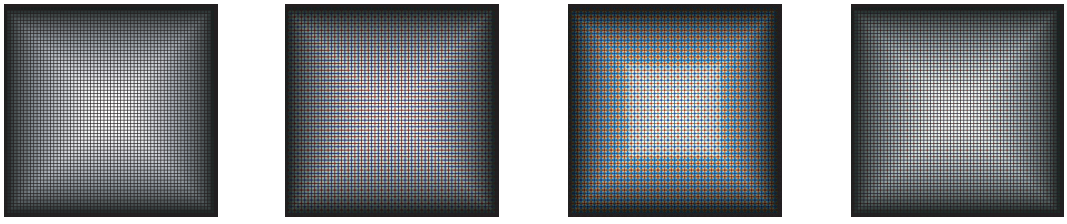

(a) (b) (c) (d)

Fig. 9 Visual appearance of the color reproduction. *Square Snake*. (a) Original. (b) ACPI. (c) PCSD. (d) Proposed.

dence of high fidelity in color reproduction of the proposed method.

The final demonstration is involved with both visual inspection and objective evaluation. It is on a synthetic image for checking the distribution of false colors. The image shown in Fig. 9[†] is achromatic and has fine mesh structure. Actually the intensity in brightness decreases from the center to outward in the anti-clockwise spiral fashion. One can see that the image in part (d) produced by the proposed method shows the appearance closest to the original.

In Fig. 10, the false color distributions are presented in the CIE 1931 chromaticity space. Since the original image is not colored by any means, only a single dot appears at the white point in the chromaticity diagram, as shown in part (a). In contrast, the chromaticity is distributed over a quite wide area in the color gamut in the chromaticity plot for the ACPI-produced image. In particular, three linear seg-

[†]*Square Snake*: http://r0k.us/graphics/pngLibrary.html

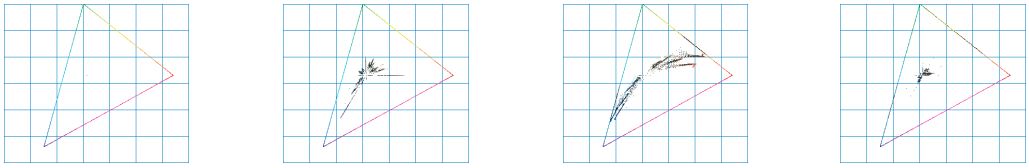

Fig. 10 False color distributions in the color gamut in the demosaicing of *Square Snake*. (a) Original. (b) ACPI. (c) PCSD. (d) Proposed.

ments toward three primary colors extends themselves long. Furthermore, there are many radial loci towards various directions. All of those chromaticity loci express false colors excepting the white point.

The false color distribution pattern is quite different in the case of PCSD. The chromaticity distribution is controlled along some curved loci toward the red and blue primaries. Unfortunately, the false colors are widely spread from the white point to the color gamut boundary.

In the case of the proposed method, most sorts of false colors are limited within a small area. This agrees with the high fidelity in its visual appearance.

6. Conclusions

In this paper, color demosaicing algorithm has been developed based on asymmetric directional interpolation and hue vector smoothing for Bayer pattern mosaic images. Experimental results have shown that the proposed method restores satisfactory images in most natural scene and portrait images in terms of subjective visual appearance and several objective metrics such as PSNR, CIELAB color difference, Munsell hue difference and CIE chromaticity.

Acknowledgement

The authors would like to thank the anonymous reviewers for their helpful comments.

References

[1] B.E. Bayer, "Color imaging array," U.S. Patent, 3 971 065, 1976.
[2] D.R. Cok, "Signal processing method and apparatus for producing interpolated chrominance values in a sampled color image signal," U.S. Patent, 4 642 678, 1987.
[3] W.T. Freeman, "Method and apparatus for reconstructing missing color samples," U.S. Patent, 4 774 565, 1988.
[4] C.A. Laroche and M.A. Prescott, "Apparatus and method for adaptively interpolating a full color image utilizing chrominance gradients," U.S. Patent, 5 373 322, 1994.
[5] J.F. Hamilton and J.E. Adams, "Adaptive color plane interpolation in single sensor color electronic camera," U.S. Patent, 5 629 734, 1997.
[6] R. Kimmel, "Demosaicing: Image reconstruction from color CCD samples," IEEE Trans. Image Process., vol.8, no.9, pp.1221–1228, Sept. 1999.
[7] B.K. Gunturk, Y. Altunbasak, and R.M. Mersereau, "Color plane interpolation using alternating projections," IEEE Trans. Image Process., vol.11, no.9, pp.997–1013, Sept. 2002.
[8] X. Wu and N. Zhang, "Primary-consistent soft-decision color demosaicing for digital cameras," IEEE Trans. Image Process., vol.13, no.9, pp.1263–1274, Sept. 2004.
[9] Y. Takahashi, H. Kikuchi, S. Muramatsu, Y. Abe, and N. Mizutani, "A proposal of demosaicing and its iteration using asymmetric average interpolation," IEICE Signal Processing Symp., D3-4, pp.1–6, Yatsugatake, Nov. 2004.
[10] Y. Takahashi, H. Kikuchi, S. Muramatsu, Y. Abe, and N. Mizutani, "A new color demosaicing method using asymmetric average interpolation and its iteration," IEICE Trans. Fundamentals, vol.E88-A, no.8, pp.2108–2116, Aug. 2005.
[11] Y. Takahashi, H. Kikuchi, S. Muramatsu, Y. Abe, and N. Mizutani, "A proposal of demosaicing and its iteration using asymmetric average interpolation," IEICE Signal Processing Symp., D3-3, pp.1–6, Kochi, Nov. 2005.
[12] Y. Takahashi, H. Kikuchi, S. Muramatsu, Y. Abe, and N. Mizutani, "Iterative asymmetric average interpolation for color demosaicing of single-sensor digital camera data," IS&T/SPIE Electronic Imaging Symp., 6069-7, pp.1–10, San Jose, Jan. 2006.
[13] K. Hiraki, Y. Takahashi, H. Kikuchi, and S. Muramatsu, "Color demosaicing using edge directed interpolation and hue-gradient smoothing," ITE Technical Report, vol.29, no.74, pp.37–40, Dec. 2005.
[14] K. Hiraki, Y. Takahashi, H. Kikuchi, and S. Muramatsu, "A study on a color demosaicing using hue transition restoration," Picture Coding Symposium of Japan, P5-01, Shuzenji, Nov. 2006.
[15] Y. Takahashi, K. Hiraki, H. Kikuchi, and S. Muramatsu, "Color demosaicing using asymmetric average interpolation and hue-transition smoothing," IEICE the 20th Workshop on Circuits and Systems in Karuizawa, Bd1-2-3, pp.167–172, Karuizawa, April 2007.
[16] M. Miyahara and I. Yoshida, "A mathematical transformation method of color data (R,G,B) to (H,V,C)," J. ITE, vol.43, no.10, pp.1129–1136, Oct. 1989.
[17] Y. Nayatani, Industrial Color Science, Asakura Shoten, Tokyo, 1980.
[18] J. Yamauchi and T. Kanazawa, ed., Handbook of Color Science, Nihon Shikisai-gakkai, University of Tokyo Press, Tokyo, 1980.
[19] G. Wyszecki and W.S. Stiles, Color Science: Concepts and Methods, Qualitative Data and Formulae, 2nd ed., John Wiley, New York, 1992.
[20] Y. Miyake, Analysis and Evaluation of Digital Color Images, University of Tokyo Press, Tokyo, 2000.
[21] A. Bovik, ed., Handbook of Image and Video Processing, Academic Press, San Diego, 2000.
[22] R. Ramanath, W.E. Snyder, and G.L. Bilbro, "Demosaicking methods for Bayer color arrays," J. Electronic Imaging, vol.11, no.3, pp.306–315, 2002.
[23] C.A.R. Hoare, "Quicksort," The Computer Journal, vol.5, pp.10–15, 1962.

Appendix: Computational Complexity

The proposed method consists of two steps: ADI (asymmet-

Table A· 1 Computational complexity per pixel.

Operations	ACPI	PCSD	ADI	HVS
additions	45	178	135	19
multiplications	20	16	20	6
absolute value	8	60	54	0
conditional branch	2	3	6	170
total	75	257	215	195

ric directional interpolation) and HVS (hue vector smoothing). ADI is an initial interpolation and HVS is an iterative process. The computational complexity is listed in Table A· 1 with a reference to PCSD and ACPI. Note that every entry shows the number of required operations per pixel, and one pixel consists of three color components of red, green, and blue. As seen in the table, ADI costs 3 times expensive as ACPI and it is inexpensive compared to PCSD. A single iteration in HVS requires additional computation, most of which consists of median filtering. The number of conditional branches for computing the median over a 5×5-block is 161 on average by Quicksort [23]. In summary, ADI is light enough as an on-line algorithm in a digital camera. HVS can be implemented separately in digital development of pictures as an off-line processing.

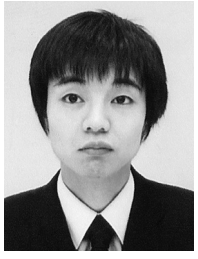

Yoshihisa Takahashi received B.E. and M.E. degrees from Niigata University in 2003 and 2005, respectively. At present, he continues his study for Ph.D. at Niigata University. His research interests include digital signal processing and image processing. He is a student member of ITE.

Kentaro Hiraki received B.E. and M.E. degrees from Niigata University in 2005 and 2007, respectively. He works at Oki Data Corporation. His research interests include digital signal processing and image processing.

Hisakazu Kikuchi (M'84) received the B.E. and M.E. degrees from Niigata University in 1974 and 1976, respectively, and Dr.Eng. degree from Tokyo Institute of Technology in 1988. From 1976 to 1979 he worked at Information Processing Systems Laboratory, Fujitsu Ltd., Tokyo. Since 1979 he has been with Niigata University, where he is a professor of electrical engineering. He was a visiting scholar at Electrical Engineering Department, University of California, Los Angeles during a year of 1992 to 1993. He holds a visiting professorship at Chongqing University of Posts and Telecommunications and Nanjing University of Information Science and Technology, both in China, since 2002 and 2005, respectively. His research interests are in the areas of image/video processing and digital signal processing as well as ultra wideband systems. Dr. Kikuchi is a member of ITE (Institute of Image Information and Television Engineers), IIEEJ (Institute of Image Electronics Engineers of Japan), JSIAM (Japan Society for Industrial and Applied Mathematics), RISP (Research Institute of Signal Processing), IEEE, and SPIE. He served the chair of Circuits and Systems Group, IEICE, in 2000 and the general chair of Digital Signal Processing Symposium, IEICE, in 1988 and Karuizawa Workshop on Circuits and Systems, IEICE, in 1996.

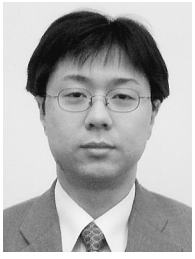

Shogo Muramatsu received B.E., M.E., and D.E. degrees in electrical engineering from Tokyo Metropolitan University in 1993, 1995, and 1998, respectively. From 1997 to 1999, he worked at Tokyo Metropolitan University. In 1999, he joined Niigata University, where he is currently an associate professor of Electrical and Electronic Engineering, Faculty of Technology. During year from 2003 to 2004, he was a visiting scientist at University of Florence, Italy. His research interests are in digital signal processing, multirate systems, image processing and VLSI architecture. Dr. Muramatsu is a member of IEEE (Institute of Electrical and Electronics Engineers, Inc.), IPSJ (Information Processing Society of Japan), ITE (Institute of Image Information and Television Engineers), and IIEEJ (Institute of Image Electronics Engineers).